Reflector design and study via conformal mappings

Luis Alemán Castañeda, Miguel Alonso

Reflector design and study via conformal mappings

Luis A. Alemán-Castañeda[a,b] and Miguel A. Alonso[a,b]

[a]The Institute of Optics, University of Rochester, Rochester NY 14627, USA
[b]Aix Marseille Univ, CNRS, Centrale Marseille, Institut Fresnel, 13013 Marseille, France

ABSTRACT

We present a new approach to relate the reflector's shape and the direction in which light gets reflected. Using a simple conformal map the reflector profile can be transformed into a curve that describes light's direction after reflection, as well as the amount of it. The method, currently limited to 2D (i.e. reflectors with a certain symmetry), can be used for both segmented and smooth reflectors, as well as with extended sources. Applications are discussed.

Keywords: Reflector Design, Illumination optics; Reflector design; Reflectors; Conformal mappings.

1. INTRODUCTION

The field of illumination optics has seen great progress[1–3] in both numerical and analytical implementations of the irradiance and/or intensity calculations given any source and a target. Early work designed reflectors through source-target maps, i.e. the correspondence between the ray angles from the source to the reflector and the target direction, and through parameters describing the system, such as the acceptance angle.[1] Modern techniques have shifted to assessing/obtaining a given irradiance or radiant intensity distributions.[4–9] The general 3D problem is governed by a nonlinear second-order Monge-Ampere equation, that in many cases has no analytical solution so numerical methods must be used. However, when there is either transnational or rotational symmetry, the system reduces to a 2D problem and analytic methods can then be used, e.g, the so-called "edge-ray",[10–14] and"flow-line"[2,15,16] methods. The approach described here falls in this category.

In many general schemes, point sources are used for designing reflectors with extended sources, such as the aforementioned edge-ray method. In addition, the supporting paraboloids[17,18] and linear programming[7,19] methods have been successful in generating the desired intensity distributions with good numerical performance, even when optimizing for extended sources. In these two methods, the reflector is subdivided into patches of paraboloids so that, based on the properties of conics, a far-field intensity distribution is tailored. Although these properties have been used extensively in non-imaging optics, the connection between their shape and the direction of light after reflection has been restricted mainly to piecewise parabolic reflectors. In a recent work,[20] we provided using conformal mappings a conceptual connection valid also in the continuous, smooth case, hence yielding a simple, visual tool for the assessment of any reflector with translational or rotational symmetry.

In this manuscript we will first motivate and introduce the conformal map studying a simple piecewise parabolic reflector. Then, in order to illustrate the simplicity and usefulness of the transformation proposed, we present a series of examples of piecewise parabolic and continuous smooth reflectors. Furthermore, we display how by employing this map, a piecewise parabolic reflector can be easily designed. Lastly, we show how extended sources can be also studied via translations.

Send correspondence to M.A.A.
L.A.A.C.: E-mail: lalemanc@ur.rochester.edu
M.A.A.: E-mail: miguel.alonso@rochester.edu

2. THE QUADRATIC CONFORMAL MAP

Let us consider a parabolic reflector of focal length f whose focus is at the origin and whose axis is at an angle β with respect the x-axis. If a point source were placed at its focus, light coming from the source would be redirected parallel to the parabola's axis. Therefore, we would like to find a map that transforms such parabolas into straight lines whose directions are related to that of the redirected light. To find this map, it is useful to write the general expressions of both the parabola and a straight line with impact parameter (distance to the origin) $\bar{d}$ and angle $\bar{\beta}$:

$$\text{parabola: } r(\theta) = f \csc^2\left(\frac{\theta-\beta}{2}\right), \qquad \text{line: } \bar{r}(\bar{\theta}) = \bar{d}\csc\left(\bar{\theta}-\bar{\beta}\right), \tag{1}$$

where an overbar is used to label quantities that refer to the straight line, to distinguish them from those of the parabola. It follows that the transformations

$$\theta = 2\bar{\theta}, \quad r = \bar{r}^2, \tag{2}$$

provide the desired map that converts a line with parameters $(\sqrt{f}, \beta/2)$ into a parabola with parameters (f, β). In other words, if we express the reflector's 2D coordinates (x, y) as a complex number $z = x + iy = r\exp(i\theta)$, the conformal map $\sqrt{z} = \sqrt{r}\exp(i\theta/2) = \bar{z} = \bar{x} + i\bar{y}$ exactly transforms parabolas with focus at the origin into straight lines, and vice-versa for $\bar{z}^2$. This map has been used in other physical contexts, e.g. to describe the caustics of structured Gaussian beams.[21] Furthermore, this map has also been used to connect Keplerian motion whose orbits are ellipses or hyperbolas centered at one of the foci, with the classical motion in a symmetric 2D quadratic (attractive or repulsive) potential whose orbits are ellipses or hyperbolas centered at the potential's center.[22–24] The case considered here of a parabola being mapped onto a straight line corresponds to the limiting case where the quadratic potential vanishes (free motion) and the Keplerian path is an escape/capture orbit.

We can then define an abstract *light space* with coordinates $(\bar{x}, \bar{y})$ in which a *light curve* exists, in contrast with the *real space* with coordinates (x, y) where the reflector exists. These spaces are linked by the map just described. As shown in Fig. 1, a reflector composed of confocal, parabolic, contiguous segments –as in the supporting paraboloids method– is transformed into a light curve which is simply a chain of straight line segments. The angle that each segment makes with the $\bar{x}$-axis is just half the angle of the reflected light with respect to the x-axis, and the angle subtended from the origin by each segment (not its length) is proportional to the corresponding redirected power.

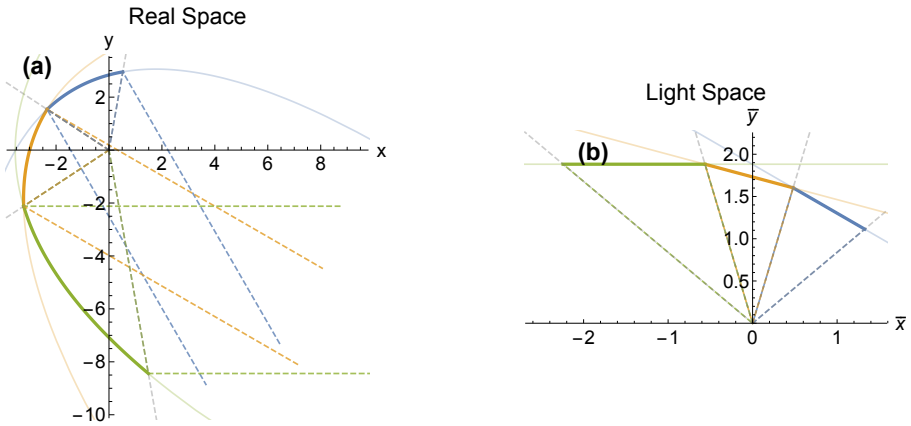

Figure 1. (a) Segmented reflector consisting of three confocal parabolic segments, each depicted in a different color. The limiting rays are shown as dashed lines. Each segment redirects the same amount of power from the source. (b) The corresponding light curve is constituted by three straight line segments at angles from the $\bar{x}$-axis equal to half the reflected light's angles from the x-axis. Although the straight line segments' lengths are different, they subtend equal angles from the origin, which are in turn half the angle subtended by the parabolic segments.

There is a subtlety to be discussed: while the conformal map $\bar{z}^2$ is well defined, the inverse map $\sqrt{z}$ is not. The problem arises due to the modular nature of the polar angle which makes $\sqrt{z}$ to be multi-valued. To avoid

this, a branch cut must be chosen, that means, selecting a range for θ. For example, when choosing $\theta \in [0, 2\pi)$, the positive real line becomes the branch cut (where the discontinuity happens). It is convenient for continuity of the light curve to choose the branch cut as the average target direction. However, the choice of branch changes neither the direction nor the subtended angles and hence is not critical.

3. PIECEWISE REFLECTORS

3.1 Reflector Design

When designing a reflector, one must choose the relationship between the ray(s) angle coming from the source toward the reflector, α, and the target direction, β, i.e., select the so-called source-target mapping. Both angles are measured with respect the optic axis which we will generally select as our x axis in our 2D representation. It is important to mention that a source-target mapping doesn't determine a unique reflector, but a family of solutions. To have a unique solution an extra parameter is needed: the distance with respect the source (origin) at a given point.

The inverse map $z = \bar{z}^2$ can be used to design reflectors from their respective light curves without explicitly tracing any rays. For a piecewise parabolic reflector the procedure is the following:

1. Choose the source range.
2. In light space this defines a range subtending just half the angle, which must be subdivided into sections depending on the fraction of energy desired for each, taking into account the source intensity distribution (e.g. if it is uniform or not).
3. In each section, draw straight-line segments oriented at half the desired target angle –this becomes the light curve.
4. Obtain the reflector by applying the map $z = \bar{z}^2$.

Note that connecting at their ends the light curve segments leads to a continuous reflector, while disconnected segments lead to Fresnel-type reflectors. In Fig. 2 we construct a continuous reflector following the former procedure.

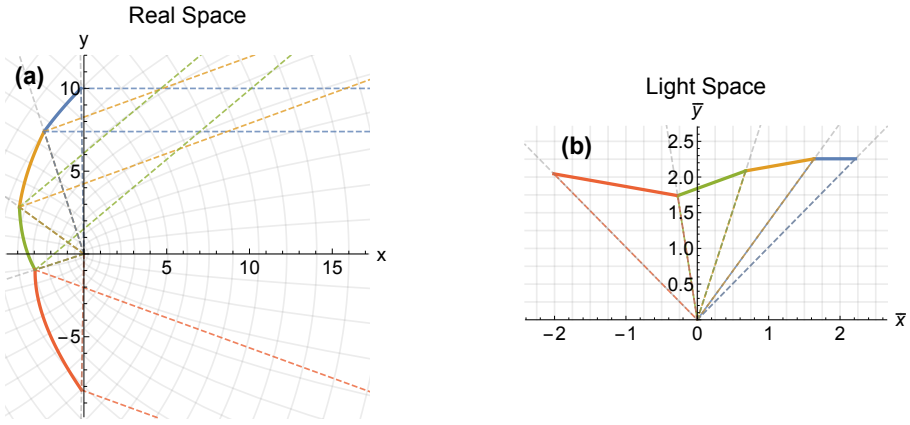

Figure 2. (a) The reflector is obtained after applying the $z = \bar{z}^2$ map. (b) Light curve construction given a source emitting uniformly and a source range $\alpha \in [90°, 270°]$, i.e. from 45° to 135° in the light space. We want to redirect 10%, 20%, 30%, and 40% of light towards $\beta = 0°,\ 20°,\ 40°$, and $-20°$ respectively, so we draw the corresponding straight-line segments oriented at half those target angles.

3.2 Reflector assessment

There are two main basic geometries of reflectors: convergent (where rays cross after reflection), and divergent (where they do not cross). Depending on the system's specifications, each geometry has advantages and disadvantages. The proposed conformal map reveals these two geometries directly, as illustrated for the two piecewise-parabolic continuous reflectors shown in Fig. 3 (with equal target and source ranges). A concave/convex light curve towards the origin implies a convergent/divergent reflector, refer to Appendix B for the proof and further discussion. Note that light curves consisting of straight segments in the same directions, each subtending the same angles, yield after the $z = \bar{z}^2$ map different reflectors with the same source and target ranges, not necessarily purely convergent or divergent, as in Fig. 2.

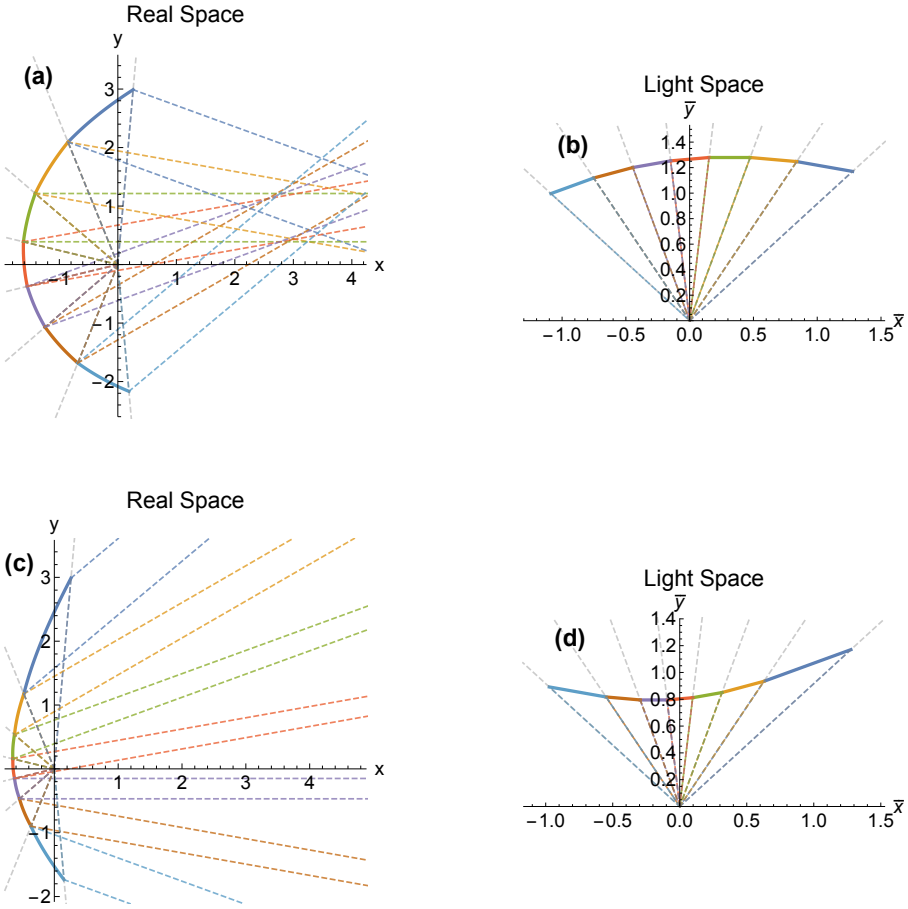

Figure 3. Two reflectors composed of six parabolic segments (a),(c) and their light curves (b),(d). The reflectors have convergent (a) and divergent (c) geometry, but have equal source and target ranges. The light curves are concave/convex towards the origin for convergent/divergent reflectors.

Let us now consider discontinuous reflectors such as piecewise-parabolic Fresnel-type reflectors, commonly used for collimation when thin reflectors are preferred due to packaging or construction limitations (although they tend to be longer). The light curve is discontinuous, like the reflector. Additionally, since typically all reflector segments have a common holder, the light curve segments should also remain attached to the mapped holder. For example, if we consider that all segments start at a line oriented at θ_c and with impact factor d, then the light curves all depart from a rectangular hyperbola (with perpendicular asymptotes) oriented at $\theta_c/2 - \pi/4$ and semi-axis $\sqrt{d}$, into which the line is transformed, see Appendix C.

On the other hand, for a collimator, which usually can be visualized as situated between two lines, its corresponding segments in light space lie between the two rectangular hyperbolas obtained from mapping them.

Figure 4 shows two reflectors and their respective light curves. All light curve segments are parallel but disconnected, i.e. their impact parameters differ. The later was expected since Fresnel-type collimators are constituted by confocal equally-oriented parabolas, but of different focal lengths. Lastly, note that while the light line segments follow a hyperbola (a convex curve), the geometry of the reflector is recovered from the angular change of the light curve: convergent if co-rotating with respect to the origin, divergent if counter-rotating, and collimating if constant. As Fig. 4 (b) shows, the light curve segments co-rotate, indicating the convergence of rays after reflection as seen in Fig. 4 (a).

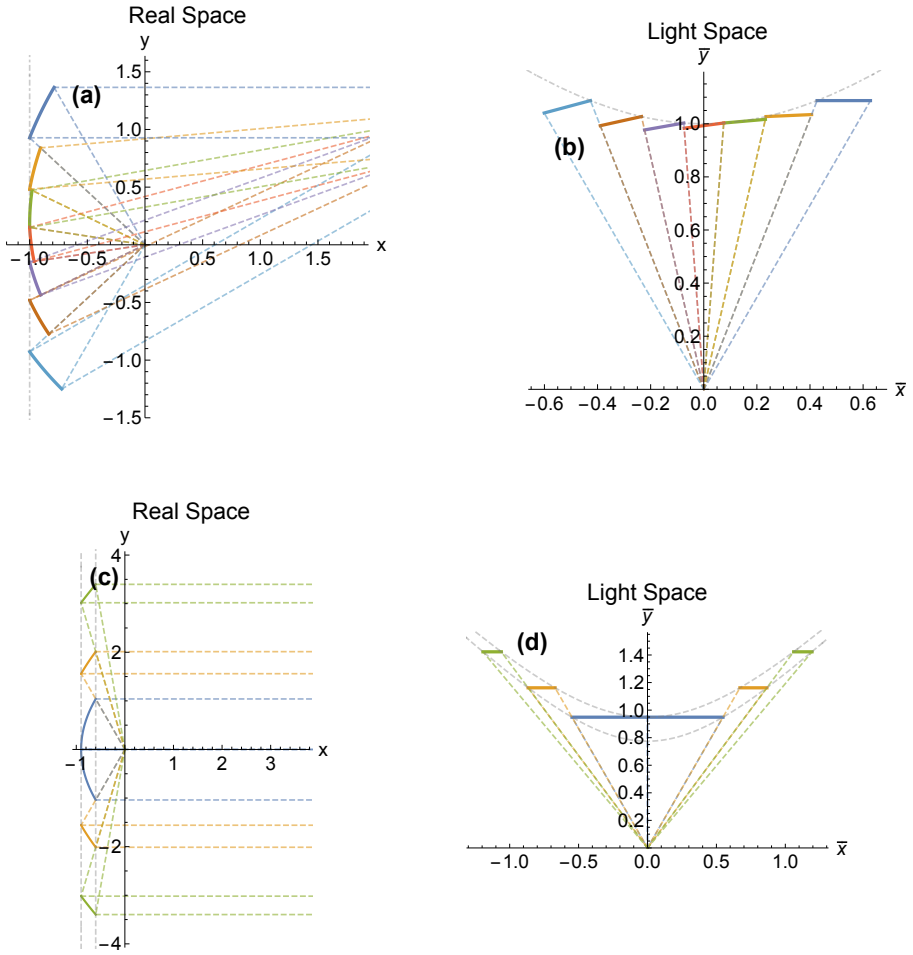

Figure 4. Segmented Fresnel-type reflectors: (a) convergent reflector with seven segments and (b) its light curve. (c) collimator, (i.e. neither divergent or convergent) with five segments and (d) its light curve. The baselines for the reflector segments map onto limiting rectangular hyperbolas for the light curves.

4. CONTINUOUS SMOOTH REFLECTORS

This approach is valid not only for segmented piecewise-parabolic reflectors, but also for continuous, smooth reflectors, which can be regarded as the limit of an infinite number of small parabolic segments (refer to Appendix A for the rigorous proof that both the reflector and the light curve are connected by the proposed transformations). In fact, for these reflectors (or segments of) that are purely converging or diverging, a polar diagram of the resulting radiant intensity can be generated from the light curve $(\bar{x}, \bar{y})$. Let these coordinates be parametrized by a variable τ. The length of a segment of this curve that spans a given infinitesimal range of directions is proportional to the local radius of curvature. This length, multiplied by an obliquity factor and divided by the distance to the origin, gives the infinitesimal angle subtended by this segment. The expression in

polar coordinates is then given by

$$(I,\theta)=\left[\frac{\dot{\bar{x}}^2+\dot{\bar{y}}^2}{\bar{x}^2+\bar{y}^2}\frac{|\bar{x}\dot{\bar{y}}-\dot{\bar{x}}\bar{y}|}{|\dot{\bar{x}}\ddot{\bar{y}}-\ddot{\bar{x}}\dot{\bar{y}}|},2\arctan\left(\frac{\dot{\bar{y}}}{\dot{\bar{x}}}\right)\right]=\left[\frac{|\dot{\bar{z}}|^2\mathrm{Im}(\dot{\bar{z}}\bar{z}^*)}{|\bar{z}|^2\mathrm{Im}(\ddot{\bar{z}}\dot{\bar{z}}^*)},2\arg(\dot{\bar{z}})\right], \tag{3}$$

where the dot denotes a derivative in τ. Note that I diverges at the light curve's inflection points, which correspond to far-field caustics. These points typically separate segments that are convergent (which form caustics between the reflector and the far field) and divergent (which form no real caustics).

In the following subsections, we will study two examples of continuous, smooth reflectors. The first consists in a comparison of circular reflectors used as collimators, in which we will use the intensity expression previously derived. The second illustrates how this method can be used also for extended sources via translations.

4.1 Study of Collimators

Consider a circular reflector of radius R, when used as a collimator at different distances from the source. This reflector is paraxially equivalent to an ideal parabolic collimator when the light source is placed half a radius away from its center ($f = R/2$). For comparison, the focal length of the parabola is set to $f = R/2$. Figure 5 shows (red curves) that the light curve in this case is considerably flat within the central region, mimicking the straight line for the ideal parabolic collimator (dashed line) within a range of source angles.

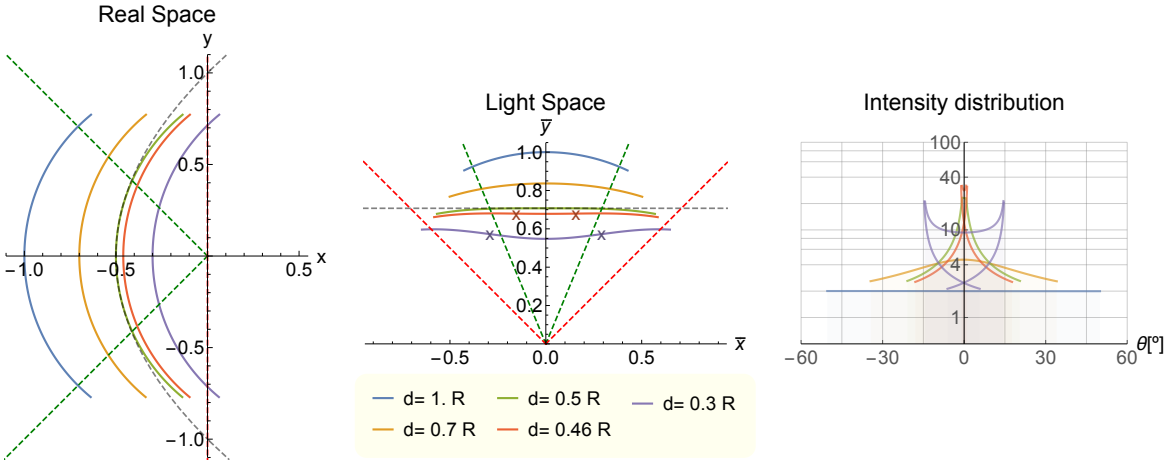

Figure 5. (a) Circular reflector of radius R at five distances d from the source. (b) Their corresponding light curves. Within $\pm 45^\circ$ of the x-axis, (green dashed lines), this profile at $d = R/2$ has good performance paraxially as a collimator. Collimation degrades at higher angles, e.g. at $\pm 90^\circ$ (red dashed lines). For a small translation, the collimation range can be extended to $\approx 67.5^\circ$. For closer positions there is clear variation from divergent to convergent behavior, the crosses indicating the inflection points (far-field caustics). (c) Logarithmic radiant intensity diagrams. These become multivalued for non-purely convergent/divergent reflectors due to the appearance of far-field caustics (cusps on the plot).

This light curve is concave away from the central region, indicating convergent behavior. The convergence at the edges can be compensated by slightly reducing the distance between the source and the reflector (this can be understood as using defocus to balance spherical aberration) at the cost of introducing divergent behavior near the axis. This can be appreciated from the light curves in Fig. 5(b) for two locations closer than the collimating paraxial position. On the other hand, the behavior is purely convergent for circular reflectors further away from the paraxial collimating position, for which Eq. (3) provides a continuous intensity diagram, as shown in Fig. 5(c).

4.2 Extended Sources

Let us finish with an example corresponding to an extended source/target: the Compound Parabolic Concentrator (CPC),[25,26] which achieves the ideal concentration limit.[2,27] A CPC consists of a planar source/concentrator and two parabolic reflectors that redirect the light from/to the opposite end of the source/concentrator at $\pi \mp \theta_c$,

where θ_c is the acceptance angle, i.e., the minimum angle from one of the corners of the source/concentrator to the upper end of the parabolic reflector (see Fig. 6). Due to the symmetry of the problem, only one of the reflectors needs to be considered.

The procedure is as follows: given the reflector shape, the origin is translated from the original focus along the extended source/concentrator, and the map $\bar{z} = \sqrt{z}$ of the reflector is then applied to reveal the direction in which light is directed after reflection. Figure 6 shows the results for six points of the extended planar concentrator and an acceptance angle of $\theta_c = \pi/3$. The first point, corresponding to the opposite end of the concentrator, leads to a perfectly straight light line at $\theta_c/2$. As the point approaches the reflector, the direction angles change mostly for small source angles (small $\bar{y}$) to a divergent geometry, whereas for larger source angles (near the edge of the reflector) the light is directed at angles close to the acceptance angle. The direction for all the positions is bounded by $\theta_c/2$, which is achieved only at the initial position. This was to be expected, since the construction of the CPC can be derived using the edge-ray technique.[2]

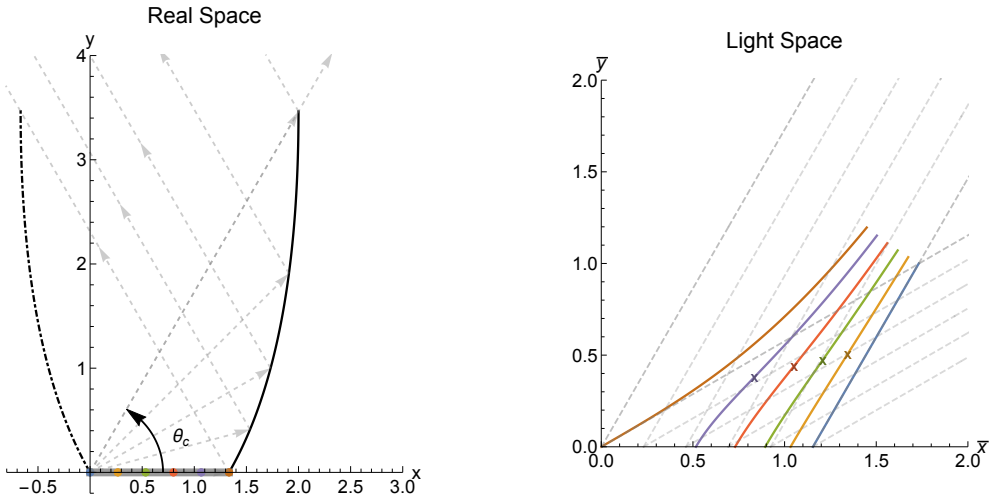

Figure 6. (a) A CPC reflector ($\theta_c = \pi/3$, $f = 1$) that collimates light from the edge source point along $\pi - \theta_c$, and six points along the extended source. (b) Light curves for these six source points. The gray-dashed lines , included for reference, indicate the directions for the acceptance angles θ_c and $\pi - \theta_c$.

5. CONCLUSIONS

The conformal maps $\bar{z}^2$ and $\sqrt{z}$ provide a simplified understanding of the relation between the reflector's shape and the light direction distribution after reflection, for both segmented and continuous, smooth reflectors. Additionally, light space can be used to design reflectors starting from their light curves, which are particularly simple for piecewise parabolic reflectors. Furthermore, from this new graphic representation, general reflector characteristics can be perceived easily even without explicitly tracing rays. For example, convergent/divergent/collimating geometries are mapped onto the convexity/concavity/straightness of the light curve. Nevertheless, light curves do not fully replace rays. For instance, cases when rays hit a reflector more than once cannot be visualized directly.

The approach is based on point-like sources which is a useful approximation in many cases and is widely used by several already-known algorithms. However, it can be applied also to extended sources by treating each point as a point source and translating the reflector before applying the map. This method is currently limited to systems whose symmetries reduce the problem to 2D, meaning that skew rays cannot yet be considered. Future work could focus on a generalization to 3D. A first (not yet successful) attempt in this direction was the use of quaternions to generalize the complex map, leading to a 4D space from which a 3D subspace can be chosen. Another possible extension is to reflectors that generate desired irradiances at finite distances, for which the map should not only reveal the direction of light but also the distance at which it focuses.

ACKNOWLEDGEMENTS

We thank Mark Dennis, Jannick Rolland, Bill Cassarly and Cristina Canavesi for separate discussions whose intersection led to this idea.

FUNDING

University of Rochester's PumpPrimer II Award (OP212647), CONACYT fellowship (LAC), Excellence Initiative of Aix-Marseille University- A*MIDEX, a French "Investissements d'Avenir" programme (MAA).

APPENDIX A. EXTENSION TO SMOOTH AND CONTINUOUS REFLECTORS

Our approach is rigorous for segmented reflectors, and to extend it to the continuum case, one could argue, heuristically, that in the limit of an infinite number of small segments it will hold. Nevertheless, we would like to show its validity more strictly, and we will do so for the z^2 inverse map, although the proof for $\sqrt{z}$ is also straight forward. Following Elmer's construction,[28,29] we can obtain a 2D curve given the map between its polar coordinate, α, and its angle of direction, $\bar{\beta}$, see Fig. 7. It can be seen that the curve would follow the relation

$$\tan\left(\bar{\omega}-\bar{\gamma}\right)=\frac{d\bar{r}}{\bar{r}d\bar{\omega}}, \tag{4}$$

from which if we do the change of variable $\bar{\omega}=\pi-\bar{\alpha}$ and use that $\bar{\gamma}=\pi/2-\bar{\beta}$ we would end up with

$$\frac{d\bar{r}}{\bar{r}}=\cot\left(\bar{\beta}-\bar{\alpha}\right)d\bar{\alpha}. \tag{5}$$

Integrating from $\bar{\theta}_0$ to $\bar{\theta}$ leads to the final expression

$$\bar{r}(\bar{\theta})=\bar{r}_0\exp\left(\int_{\bar{\theta}_0}^{\bar{\theta}}\cot\left(\bar{\beta}-\bar{\alpha}\right)d\bar{\alpha}\right), \tag{6}$$

where $\bar{r}_0$ is the initial point distance that fixes the solution.

We would like to apply z^2, i.e. $\bar{r}\to\bar{r}^2=r$ and $\bar{\theta}\to 2\bar{\theta}=\theta$, to show that the light curve is transformed into the corresponding reflector. So, squaring expression (6), renaming $r=\bar{r}^2$ along with $\beta=2\bar{\beta}$, and doing $2\bar{\alpha}=\alpha$, we get

$$r\left(2\bar{\theta}\right)=r_0\exp\left(\int_{2\bar{\theta}_0}^{2\bar{\theta}}\cot\left(\frac{\beta-\alpha}{2}\right)d\alpha\right), \tag{7}$$

where we dropped the explicit dependency of $\bar{\beta}(\alpha)$ (to ease writing). This equation is almost what we are looking for, we just have to recognize that given the doubling of the angle, now $\theta=2\bar{\theta}$, so

$$r\left(\theta\right)=r_0\exp\left(\int_{\theta_0}^{\theta}\cot\left(\frac{\beta-\alpha}{2}\right)d\alpha\right), \tag{8}$$

which is exactly the equation derived by Elmer[28] for a reflector that sends the light coming from the source at an angle α to an angle β. As shown in Fig. 7, the relation given in Eq. (4) changes for the reflector to

$$\tan\left(\frac{\omega+\beta}{2}\right)=\frac{dr}{rd\omega}, \tag{9}$$

from which, similarly, after using that $\omega=\pi-\alpha$ and integrating between θ_0 and θ, Eq. (8) can be obtained.

Additionally, it can be shown that the angle of a curve segment in the real space, ν, under the map $\sqrt{z}$ is transformed into as $\bar{\nu}=\nu-\frac{\alpha}{2}$, meaning that the angular change is given by the shrinking or expansion of the polar coordinate α, and does not depend on the original angle. Since the light curve segment is only at half of the angle in which light is reflected after hitting the reflector, the transformation leads $\nu=(\beta+\alpha)/2$, that is the same geometrical relation between the angle of incidence, the local angle of the reflector, and the angle in which light gets reflected, described in the literature[28] and discussed previously (see Fig. 7).

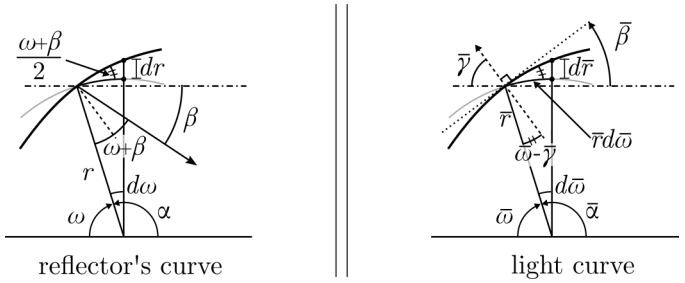

Figure 7. Schematic construction of a curve given a correspondence between its tangent angle and its polar coordinate: (left) for a reflector with source-target map $\beta(\alpha)$, the tangent angle is equal to $(\alpha+\beta)/2$; (right) for the light curve with polar angle $\bar{\alpha}$, the tangent angle is $\bar{\beta}$. Notice that for the reflector, β is negative, i.e., light is going downwards.

APPENDIX B. REFLECTORS GEOMETRY REVEALED BY THE LIGHT CURVE

Let us consider a reflector whose source-target map is given by $\beta(\alpha)$, where α is the source angle, which in our case is the polar angle. The corresponding light curve's local direction is then given by $\bar{\beta} = \beta/2$. The light curve, or some of its segments, are said to be concave/convex/straight if the angular derivative of its direction, $\partial\bar{\beta}/\partial\bar{\alpha}$, is positive/negative/zero. It follows from relation between the reflector and its light curve that

$$\frac{\partial\bar{\beta}}{\partial\bar{\alpha}} = \frac{1}{2}\frac{\partial\beta}{\partial\bar{\alpha}}. \tag{10}$$

Then, from the relation between the light space and the real space, remember $\alpha = 2\bar{\alpha}$, we finally obtain

$$\frac{\partial\bar{\beta}}{\partial\bar{\alpha}} = \frac{1}{2}\frac{\partial\beta}{\partial\alpha}\frac{\partial\alpha}{\partial\bar{\alpha}} = \frac{\partial\beta}{\partial\alpha}. \tag{11}$$

This was the missing link, since a reflector's geometry, or some of its segments', is considered converging/diverging/collimating if the angular derivative of its source-target mapping, $\partial\beta/\partial\alpha$, is positive/negative/zero.

APPENDIX C. TRANSFORMATION OF STRAIGHT LINES

A line after the conformal mapping $\sqrt{z}$ is transformed into a rectangular hyperbola, whose asymptotes make an angle of $\pi/2$. This can be understood intuitively: given that the light-curve is parallel to the reflected rays under $\sqrt{z}$, we know the asymptotic reflection from a line (flat surface) will be parallel to it, i.e.,$-\pi/2$ and $\pi/2$ with respect to its normal, giving a total angle of π in the real space, but only half in the light space. Being more rigorous, consider a line in the real space with parameters (d, β) and its transformation,

$$r_{\text{line}}(\theta) = d\csc(\theta-\beta), \qquad \bar{r}_{\text{hyp.}}(\bar{\theta}) = \sqrt{d}\sqrt{\csc(2\bar{\theta}-\beta)}. \tag{12}$$

Then, consider the canonical hyperbola given by

$$\frac{\bar{x}^2}{a^2} - \frac{\bar{y}^2}{b^2} = 1, \tag{13}$$

where a and b stand for its semi axis lengths. In the case of a rectangular hyperbola, $a = b$, hence, changing to polar coordinates and solving for $\bar{r}$,

$$\bar{r}(\bar{\theta}) = a\sqrt{\sec 2\theta}. \tag{14}$$

If we wanted it to have an arbitrary orientation φ, we just need to let the angle be $\theta - \varphi$, and so the final expression becomes

$$\bar{r}(\bar{\theta}) = a\sqrt{\csc(2\bar{\theta} - (2\varphi - \pi/2))}, \tag{15}$$

meaning that the orientation of the rectangular hyperbola will be given by $\varphi = \beta/2 + \pi/4$.

APPENDIX D. FORMULAE OF CONIC COLLIMATORS

Lastly, it will be of use to derive the polar equation of a conic translated so that it is acting as a collimator. For example, in the case of a circle, this occurs when the translation was by half its radius, $R/2$. In general, we need to remember that the radius of curvature at the vertex of any conic is given by the semi latus rectum, ℓ, and so the translation required is given by $\ell/2$, so

$$\frac{x-(\ell/2)}{a^2} \pm \frac{y^2}{b^2} = 1, \tag{16}$$

where, a and b stand for the semi axis lengths of the conic. Then, using the fact that $\ell = b^2/a$, and using carefully the eccentricity definition, as well as keeping the possible sign changes from hyperbola to ellipse, we have that $\pm b^2 = a^2 - c^2 \implies \pm b^2/a^2 = (1-e^2)$, the equation for any conic becomes

$$(1-e^2)x^2 + y^2 - \ell(1+e^2)x - \frac{\ell^2}{4}(3+e^2) = 0. \tag{17}$$

Notice that the $\pm$ symbol disappears of the expression giving a unique formula, and more importantly, the semi latus rectum, ℓ, as well as the eccentricity, e, are preferred to express a conic since the conic constants a, b, and c can get undetermined in certain scenarios, e.g. for the parabola. Lastly, we need to convert to polar coordinates, obtaining

$$r(\theta) = \ell \left\{ \frac{(1+e^2)\cos(\theta) + \sqrt{(1-e^2)\cos^2(\theta) + (3+e^2)}}{2[1-e^2\cos^2(\theta)]} \right\}. \tag{18}$$

If we wanted it to have an arbitrary orientation ϕ, we just need to let the angle be $\theta - \phi$. The respective light curve can be obtained by doing $\theta \mapsto 2\bar{\theta}$ and $r \mapsto \bar{r}^2$.

REFERENCES

[1] Winston, R., [*Selected Papers on Nonimaging Optics*], SPIE Milestone Series, SPIE (1995).

[2] Winston, R., Jiang, L., and Ricketts, M., "Nonimaging optics: a tutorial," *Adv. Opt. Photon.* **10**(2), 484–511 (2018).

[3] Wu, R., Feng, Z., Zheng, Z., Liang, R., Benítez, P., Miñano, J., and Duerr, F., "Design of freeform illumination optics," *Laser and Photonics Reviews* (2018).

[4] Miñano, J. C. and González, J. C., "New method of design of nonimaging concentrators," *Appl. Opt.* **31**(16), 3051–3060 (1992).

[5] Ries, H. and Muschaweck, J., "Tailored freeform optical surfaces," *J. Opt. Soc. Am. A* **19**(3), 590–595 (2002).

[6] Oliker, V., "Mathematical aspects of design of beam shaping surfaces in geometrical optics," in [*Trends in Nonlinear Analysis*], Kirkilionis, M., Krömker, S., Rannacher, R., and Tomi, F., eds., 193–224, Springer Berlin Heidelberg, Berlin, Heidelberg (2003).

[7] Canavesi, C., Cassarly, W. J., and Rolland, J. P., "Target flux estimation by calculating intersections between neighboring conic reflector patches," *Opt. Lett.* **38**(23), 5012–5015 (2013).

[8] Wester, R., Müller, G., Völl, A., Berens, M., Stollenwerk, J., and Loosen, P., "Designing optical free-form surfaces for extended sources," *Opt. Express* **22**(S2), A552–A560 (2014).

[9] Hirst, A., Muschaweck, J., and Benítez, P., "Fast, deterministic computation of irradiance values using a single extended source in 3d," *Opt. Express* **26**(14), A651–A656 (2018).

[10] Gordon, J. M. and Ries, H., "Tailored edge-ray concentrators as ideal second stages for fresnel reflectors," *Appl. Opt.* **32**(13), 2243–2251 (1993).

[11] Davies, P. A., "Edge-ray principle of nonimaging optics," *J. Opt. Soc. Am. A* **11**(4), 1256–1259 (1994).

[12] Ries, H. R. and Winston, R., "Tailored edge-ray reflectors for illumination," *J. Opt. Soc. Am. A* **11**(4), 1260–1264 (1994).

[13] Rabl, A. and Gordon, J. M., "Reflector design for illumination with extended sources: the basic solutions," *Appl. Opt.* **33**(25), 6012–6021 (1994).

[14] Ong, P. T., Gordon, J. M., and Rabl, A., "Tailored edge-ray designs for illumination with tubular sources," *Appl. Opt.* **35**(22), 4361–4371 (1996).

[15] Lun Jiang, R. W., "Thermodynamic origin of nonimaging optics," *Journal of Photonics for Energy* **6**, 6 – 6 – 11 (2016).

[16] Lun Jiang, R. W., "Flow line asymmetric nonimaging concentrating optics," *Proc. SPIE* **9955**, 9955 – 9955 – 8 (2016).

[17] Kochengin, S. A. and Oliker, V. I., "Determination of reflector surfaces from near-field scattering data," *Inverse Problems* **13**(2), 363–373 (1997).

[18] Canavesi, C., Cassarly, W. J., and Rolland, J. P., "Direct calculation algorithm for two-dimensional reflector design," *Opt. Lett.* **37**(18), 3852–3854 (2012).

[19] Canavesi, C., Cassarly, W. J., and Rolland, J. P., "Observations on the linear programming formulation of the single reflector design problem," *Opt. Express* **20**(4), 4050–4055 (2012).

[20] Alemán-Castañeda, L. A. and Alonso, M. A., "Study of reflectors for illumination via conformal maps," *Opt. Lett.* **44**(15), 3809–3812 (2019).

[21] Alonso, M. A. and Dennis, M. R., "Ray-optical poincare sphere for structured gaussian beams," *Optica* **4**, 476–486 (Apr 2017).

[22] Rockmore, R., "On the isotropic oscillator and the hydrogenic atom in classical and quantum mechanics," *American Journal of Physics* **43**(1), 29–32 (1975).

[23] Mittag, L. and Stephen, M. J., "Conformal transformations and the application of complex variables in mechanics and quantum mechanics," *American Journal of Physics* **60**(3), 207–211 (1992).

[24] Grant, A. K. and Rosner, J. L., "Classical orbits in power-law potentials," *American Journal of Physics* **62**(4), 310–315 (1994).

[25] Winston, R., "Light collection within the framework of geometrical optics∗," *J. Opt. Soc. Am.* **60**(2), 245–247 (1970).

[26] Winston, R., "Principles of solar concentrators of a novel design," *Solar Energy* **16**(2), 89 – 95 (1974).

[27] Miñano, J. C., "Effect of restricting the exit angle on the limit of concentration for cylindrical concentrators," *Appl. Opt.* **23**(24), 4554–4559 (1984).

[28] Elmer, W. B., [*The Optical Design of Reflectors*], John Wiley & Sons, 2nd ed. (1980).

[29] Winston, R., Miñano, J. C., Benitez, P., Bortz, W., Shatz, N., and Bortz, J., [*Nonimaging Optics*], Optics and Photonics, Elsevier Science (2005).